31st International Conference Nuclear Energy for New Europe
NENE 2022 September 12-15 PORTOROŽ SLOVENIA

Maximum Required Excess Reactivity Due To Xe-135 Poisoning

Blaž Levpušček
University of Ljubljana, Faculty of Mathematics and Physics
Jadranska ulica 19
1000, Ljubljana, Slovenia
bl6386@student.uni-lj.si

Gašper Žerovnik, Luka Snoj
Jožef Stefan Institute
Jamova cesta 39
1000, Ljubljana, Slovenia
gasper.zerovnik@ijs.si, luka.snoj@ijs.si

ABSTRACT

As the share of renewable energy sources increases and production of electricity via fossil fuels is expected to decrease there is a new challenge presented to the nuclear power plants. They need to become more flexible and indulge in the so-called load following mode of operation to compensate for intermittent production of solar and wind energy. This paper presents how different fuel parameters affect negative reactivity after shutdown due to the build-up of ^{135}Xe. Xenon poisoning is one of the limiting factors in load following capabilities of the nuclear power plants, thus reducing its effect will allow power plants to run for longer periods of time. Burnup calculations were made using the computer code Serpent. Two different types of fuel were tested, MOX and UO_2. Three different initial enrichments (IEs) of UO_2 fuel were used, fuel to moderator ratio was varied and boron concentration was changed. It was observed that MOX fuel causes significantly lower ^{135}Xe build-up than the reference UO_2 fuel, which is beneficial for load following. Higher IEs result in lower ^{135}Xe build-up. Shifting the neutron spectrum towards higher energies, either by reducing moderator:fuel ratio or by introducing higher concentrations of boron reduces ^{135}Xe build-up.

1 INTRODUCTION

Due to increasing fraction of electricity being generated via intermittent renewable energy sources such as solar and wind energy, a flexible source like nuclear energy must compensate for the difference between electricity consumption and production from renewable energy sources. This kind of operation of a power plant is called load following mode. Since the fraction of both nuclear and renewable energies was, or still is, low, the capability of nuclear energy for load following was of limited importance [1]. As nuclear energy is practically the only zero carbon energy source that can act on demand it will have a more significant role and consequently greater responsibility for load following operation.

Load following mode of operation of nuclear power plants also comes with some challenges. One of them is ^{135}Xe build-up, also referred to as "poisoning", after shutdown or an extended period of power reduction [2]. If a nuclear reactor shuts down after a long period of operation at full power, the build-up of ^{135}Xe may prevent a start-up of the reactor if the available excess reactivity is insufficient.

This paper focuses on observing how different parameters such as fuel type, moderator to fuel ratio and boron concentration affect maximum negative reactivity that is induced after reactor shutdown in relation to fuel burnup (BU).

2 ASSUMPTIONS

The Serpent model was heterogeneous 2D infinite reactor. It was assumed that the parameters in one fuel element were representative of the whole 2D reactor. The parameters were homogenised by averaging across the whole neutron energy spectrum and reactor core volume. Initial condition was set to be equilibrium at full power. It was assumed that the required excess reactivity equals the maximum difference between the negative feedback reactivity from ^{135}Xe after shutdown and negative feedback reactivity from ^{135}Xe in equilibrium at full power.

3 DERIVATION

The balance equations for ^{135}Xe and ^{135}I concentrations can be expressed as [3]:

$$\frac{\mathrm{d}I}{\mathrm{d}t} = \gamma_I R_f - \lambda_I I, \qquad \frac{\mathrm{d}X}{\mathrm{d}t} = \gamma_X R_f + \lambda_I I - \lambda_X X - \frac{\bar{\sigma}_{a,X} X}{\Sigma_f} R_f, \tag{1}$$

and

$$R_f = \int \varphi(E) \sum_j N_j \sigma_{f,j}(E) = \Sigma_f \phi, \tag{2}$$

where I and X are the number densities of ^{135}I and ^{135}Xe respectively, γ_I is cumulative ^{135}I fission yield (fission rate weighted average over actinides), γ_X is independent ^{135}Xe fission yield (fission rate weighted average over actinides), λ_I is ^{135}I decay constant (2.93×10^{-5} s^{-1}), λ_X is ^{135}Xe decay constant (2.11×10^{-5} s^{-1}), $\bar{\sigma}_{a,X}$ is spectrum-averaged neutron capture cross section in ^{135}Xe, Σ_f is spectrum-averaged homogenised macroscopic neutron induced fission cross section, $\sigma_{f,j}(E)$ is neutron induced fission cross section of nuclide j, N_j is number density of nuclide j, $\varphi(E)$ is neutron flux spectrum and ϕ is neutron flux (energy integrated flux spectrum).

In general, the influence of ^{135}Xe on reactivity can be expressed as:

$$\Delta\rho_X = -\frac{R_X}{\nu R_f} = -\frac{\bar{\sigma}_{a,X}\phi X}{\bar{\nu}\Sigma_f}, \tag{3}$$

where $\bar{\nu}$ is the weighted average of the fission neutron multiplicity over actinide fission rates and neutron spectrum, and R_X is the neutron capture rate in ^{135}Xe.

Concentrations of ^{135}Xe and ^{135}I in equilibrium are

$$X_\infty = \frac{(\gamma_X + \gamma_I) R_f}{\lambda_X + R_f \frac{\bar{\sigma}_{a,X}}{\Sigma_f}} = \frac{(\gamma_X + \gamma_I) R_f}{\tilde{\lambda}_X}, \qquad I_\infty = \frac{\gamma_I R_f}{\lambda_I}, \tag{4}$$

where $\tilde{\lambda}_X = \lambda_X + \bar{\sigma}_{a,X}\phi$. Maximum ^{135}Xe concentration after shutdown can be calculated using equations (1) and (4). It will be reached when the rate of change of concentration of ^{135}Xe will equal zero.

Maximum ^{135}Xe concentration can be inserted into equation (3). An equation for maximum difference in negative feedback reactivity due to ^{135}Xe build-up is derived:

$$\delta\rho_X = \Delta\rho_{X_{max}} - \Delta\rho_{X_\infty}, \qquad K = \frac{\lambda_I/\lambda_X}{\frac{\lambda_I-\lambda_X}{\tilde{\lambda}_X}\frac{C_X}{C_I}+1} > 1, \tag{5}$$

$$\delta\rho_X = -\frac{\bar{\sigma}_{a,X}\phi}{\bar{\nu}}\left[\frac{C_I}{\lambda_I-\lambda_X}\left(K^{-\frac{\lambda_X}{\lambda_I-\lambda_X}} - K^{-\frac{\lambda_I}{\lambda_I-\lambda_X}}\right) + \frac{C_X}{\tilde{\lambda}_X}\left(K^{-\frac{\lambda_X}{\lambda_I-\lambda_X}} - 1\right)\right], \tag{6}$$

where C_I and C_X are cumulative ^{135}I and ^{135}Xe fission yields respectively.

4 DEFINITION OF (SOME) INTEGRAL PARAMETERS

The system-dependent parameters are: cumulative fission yield for ^{135}I (C_I) and ^{135}Xe (C_X), neutron flux (ϕ), average neutron capture cross section of ^{135}Xe ($\bar{\sigma}_{a,X}$) and the average fission neutron multiplicity ($\bar{\nu}$). In general, cross sections have to be averaged over neutron energy and volume:

$$\bar{\sigma} = \int \varphi(E,\vec{r})\sigma(E)\mathrm{d}E\frac{\mathrm{d}V}{V}\Big/\phi, \qquad \phi = \int \varphi(E,\vec{r})\mathrm{d}E\frac{\mathrm{d}V}{V}. \tag{7}$$

In this case,

$$\bar{\sigma}_{a,X}\phi = \int \varphi(E,\vec{r})\sigma_{a,X}(E)\mathrm{d}E\frac{\mathrm{d}V}{V}. \tag{8}$$

Effective cumulative fission yields C_i (in this case $i \in \{I, X\}$) are weighted averages over fission rates of actinides j in fuel:

$$C_i = \int \varphi(E,\vec{r})\sum_j C_{i,j}N_j(\vec{r})\sigma_{f,j}(E)\mathrm{d}E\mathrm{d}V\Big/\int \varphi(E,\vec{r})\sum_j N_j(\vec{r})\sigma_{f,j}(E)\mathrm{d}E\mathrm{d}V, \tag{9}$$

where it is assumed the cumulative fission yields have a weak dependence on neutron energy.

Finally, the fission neutron multiplicity $\bar{\nu}$ is averaged over over fission rates of actinides j in fuel, over neutron energy and over volume:

$$\bar{\nu} = \int \varphi(E,\vec{r})\sum_j \nu_j(E)N_j(\vec{r})\sigma_{f,j}(E)\mathrm{d}E\mathrm{d}V\Big/\int \varphi(E,\vec{r})\sum_j N_j(\vec{r})\sigma_{f,j}(E)\mathrm{d}E\mathrm{d}V, \tag{10}$$

where $\nu_j(E)$ is the fission neutron multiplicity of nuclide j at incident neutron energy E.

5 PARAMETRIC STUDY

A simplified PWR 2D fuel single pin model with reflective boundary conditions was used in Serpent [4](3x3 area shown on figure 1). The reference model has the following characteristics:

- Dimensions: fuel radius 0.4095 cm, cladding inner/outer radius 0.418/0.475 cm, rod pitch 0.63 cm.
- Materials: fuel UO_2/MOX ($\rho = 10.9698$ g/cm^3, $T = 900$ K), cladding Zircaloy-4 ($\rho = 6.56$ g/cm^3, $T = 600$ K), coolant water ($\rho = 0.6747$ g/cm^3, $T = 600$ K, no boron).

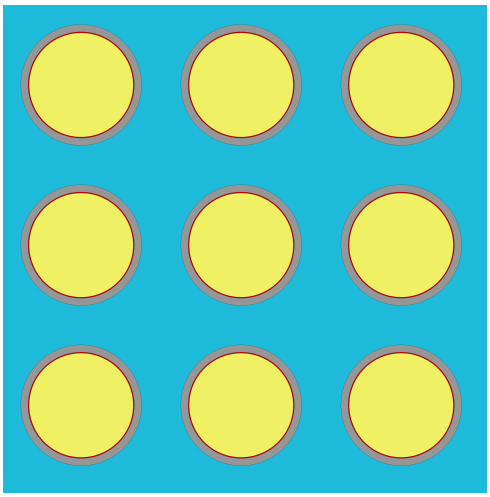

Figure 1: Figure depicts 3x3 area of 2D Serpent model. Yellow area represents fuel, red helium, grey zircaloy-4 cladding and blue water.

- Operation conditions: the fuel pin irradiated at a constant linear power density 250 kW/cm.
- Numerical parameters:
  - 4 radial depletion zones within fuel pin.
  - Bateman equation solver: predictor-corrector with 10 substeps, linear extrapolation-interpolation.
  - Time steps: 4×25 d, 4×50 d, $n \times 100$ d.
  - 1000 active neutron cycles per time step, 10000 neutron histories per cycle.
- Nuclear data: ENDF/B-VII.1 library [5].

5.1 UO_2 vs. MOX fuel

Reference UO_2 fuel with $4\,\%$ initial enrichment (IE), i.e. 4 wt.$\,\%$ ^{235}U in U and MOX fuel with 3.36 wt.$\,\%$ Pu/(U+Pu) and a typical isotopic composition were studied. Entire fuel compositions are given in Table 1.

It can clearly be observed from figure 2 that from the ^{135}Xe poisoning aspect the MOX fuel is significantly more beneficial for load-following operations than UO_2 fuel. This difference is especially important towards the end of the fuel cycle, i.e. at high burnups, where the excess reactivity is low. This may lead to (at least partial) restrictions of the load-following capabilities. This is partly a consequence of a higher fission neutron multiplicity of Pu isotopes compared to ^{235}U shown in figure 2. Also, the average recoverable energy per fission is higher for Pu isotopes which results in less fission events at a fixed power density compared to ^{235}U. Additionally, the spectrum averaged ^{135}Xe neutron capture cross section shown in figure 3, which directly affects the magnitude of the reactivity feedback, is significantly lower for the MOX fuel. This is partially compensated by a higher ^{135}Xe cumulative fission yield in Pu isotopes compared to ^{235}U shown in figure 3, however not enough to overweigh the total reactivity feedback effect.

Table 1: Actinide composition of the fresh reference UO_2 and MOX fuel.

Nuclide	Weight fraction in UO_2 fuel	Weight fraction in MOX fuel
^{234}U	$3.76 \cdot 10^{-4}$	/
^{235}U	$4.00 \cdot 10^{-2}$	$2.30 \cdot 10^{-3}$
^{236}U	$8.00 \cdot 10^{-6}$	/
^{238}U	$9.56 \cdot 10^{-1}$	$9.64 \cdot 10^{-1}$
^{238}Pu	/	$3.50 \cdot 10^{-4}$
^{239}Pu	/	$2.07 \cdot 10^{-2}$
^{240}Pu	/	$7.90 \cdot 10^{-3}$
^{241}Pu	/	$3.00 \cdot 10^{-3}$
^{242}Pu	/	$1.30 \cdot 10^{-3}$
^{241}Am	/	$3.50 \cdot 10^{-4}$

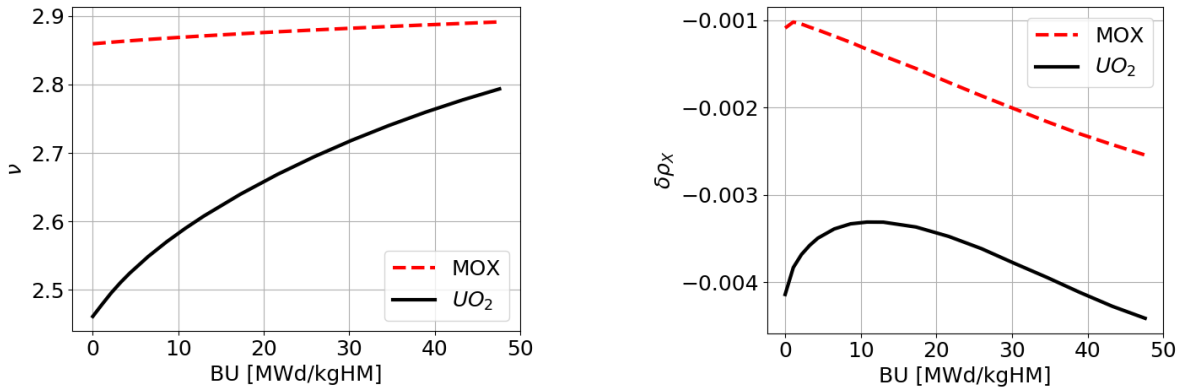

Figure 2: Average fission neutron multiplicity $\bar{\nu}$ (left) and the difference between the maximum and equilibrium ^{135}Xe reactivity feedback effect $\delta\rho_X$ (right) as a function of fuel BU for reference UO_2 and MOX cases.

5.2 Dependence on initial ^{235}U enrichment

The initial ^{235}U enrichment (IE) was varied to observe the dependence of $\delta\rho_X$ on fresh fuel isotopic U composition.

It can be observed from figure 4 that from the ^{135}Xe poisoning aspect a higher IE causes a smaller negative reactivity feedback effect due to ^{135}Xe build-up. This difference is almost independent of burnup, however due to lower excess reactivity towards the end of the fuel cycle it is gaining on importance with burnup. The main driver behind the smaller ^{135}Xe feedback reactivity effect at higher IE is a lower neutron flux at a given power density, which is a consequence of a higher macroscopic fission cross section. Additional contributors to this difference are lower ^{135}I and ^{135}Xe cumulative fission yields at higher burnups, which are caused by a lower $^{238}\text{U} \rightarrow {}^{239}$Pu conversion factor at higher IE, and a lower spectrum averaged ^{135}Xe neutron capture cross section depicted on figure 4. This is partially compensated by a lower average fission neutron multiplicity at higher burnups, which is also a consequence of a smaller build-up of ^{239}Pu. Additionally, higher IE automatically corresponds to higher excess reactivity which enables higher average burnups and consequently longer fuel cycles. A longer fuel cycle means that the fraction of the time where restrictions on load-following operations might apply, is lower. It can therefore be concluded that higher IE is beneficial for load-following operations.

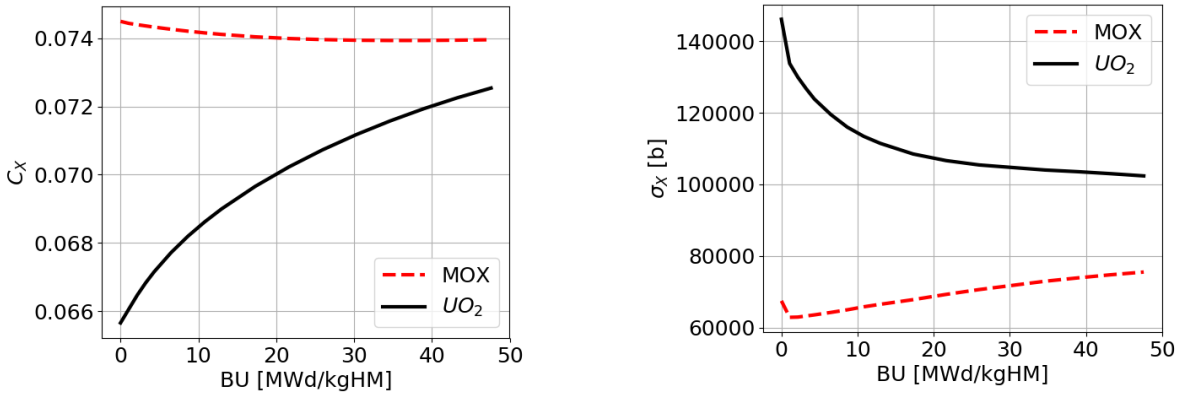

Figure 3: Cumulative fission yields of ^{135}Xe (left) and neutron spectrum averaged neutron capture cross section $\bar{\sigma}_{a,X}$ in ^{135}Xe (right) as a function of fuel BU for reference UO_2 and MOX cases.

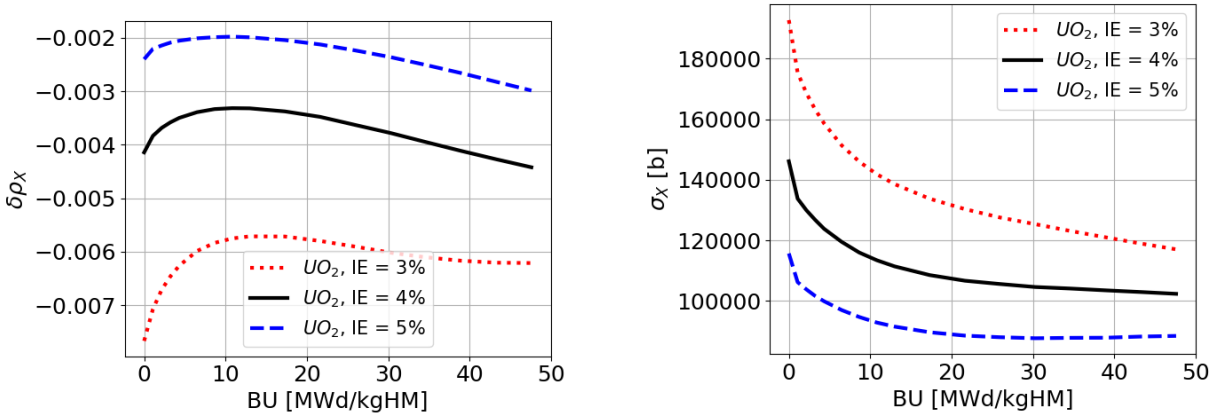

Figure 4: The difference between the maximum and equilibrium ^{135}Xe reactivity feedback effect $\delta\rho_X$ (left) and the neutron spectrum averaged neutron capture cross section $\bar{\sigma}_{a,X}$ in ^{135}Xe (right) as a function of fuel BU for different IE.

5.3 Dependence on H:fuel atom ratio

The ratio between the moderator (H atoms) and fuel number density was varied by changing the distance between fuel rods. The extreme cases were fuel rods touching and fuel rods being separated by diameter of one fuel rod. The H:fuel ratio is presented in form of moderator/fuel surface ratio.

Increase in H:fuel ratio leads to increase in neutron moderation and a higher peak in neutron spectrum around the thermal energy. Neutron spectra for both types of fuel is depicted in figure 5.

Relation between $\delta\rho_{Xe}$ and burnup is depicted in figure 6 for different H:fuel ratios. A similar behaviour of $\delta\rho_{Xe}$ in MOX and UO_2 is observed. Larger moderator:fuel ratio leads to more ^{135}Xe poisoning especially at higher burnups. One reason for this is a higher neutron spectrum averaged neutron capture cross section for ^{135}Xe at higher ratios which in turn is due to increase in thermal neutron peak. Fuel with a higher H:fuel ratio has a lower concentration of fissile nuclides such as ^{235}U and ^{239}Pu at the end of the burning cycle than fuel with a lower H:fuel ratio. This means that more fission events had to occur in highly moderated fuel which lead to more ^{135}Xe being generated. It has been observed, that lower thermal neutron peak and lower amount of fission events would lead to less ^{135}Xe poisoning, especially at higher burnups.

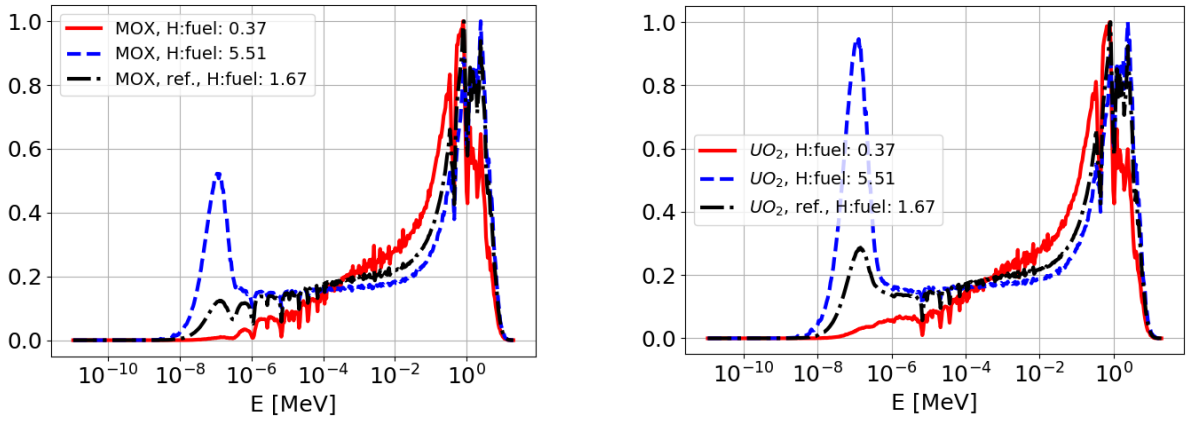

Figure 5: Neutron spectrum for MOX (left) and UO_2 (right) fuel in relation to fuel BU.

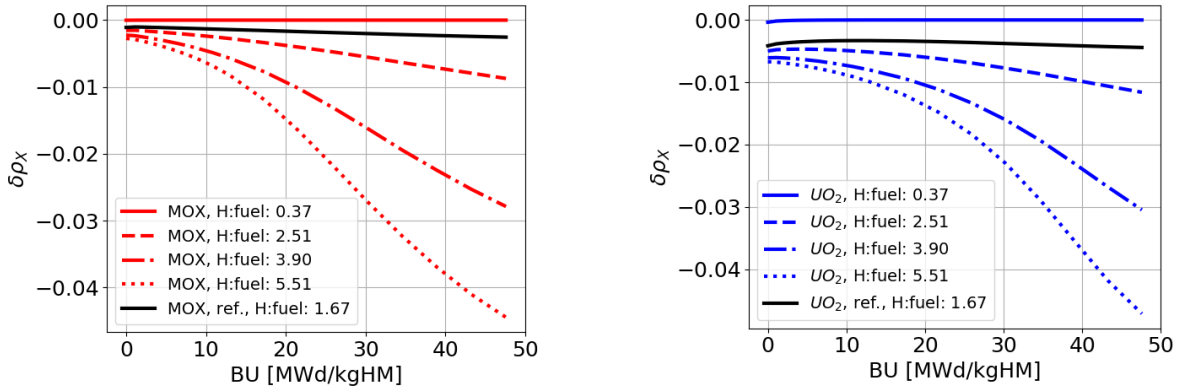

Figure 6: The difference between the maximum and equilibrium ^{135}Xe reactivity feedback effect $\delta\rho_{Xe}$ for MOX (left) and UO_2 (right) fuel in relation to fuel BU.

This means that reactors with a harder neutron spectrum would have advantage over thermal reactors at being able to operate in load following mode considering ^{135}Xe poisoning.

5.4 Dependence on initial boron concentration

An amount of natural boron was added to water. Calculations were performed for 1000 ppm and 2000 ppm of boron in water independent of burnup. A semi-realistic model was also used where boron concentration was varied so that $k_{eff} = 1$ for as long as possible. Boron concentration and k_{eff} dependencies for this semi-realistic case are shown on figure 7.

Addition of boron decreases the absolute value of the negative reactivity due to ^{135}Xe build-up. This can be seen in figure 8. More boron in moderator means more thermal neutron absorptions. Shifting of the spectrum leads to a lower absorption cross section of ^{135}Xe σ_{Xe}, depicted in figure 8. Therefore, less ^{135}Xe is produced and the negative feedback reactivity due to it is lower. Boron reduces negative reactivity more for UO_2 fuel than for MOX fuel relative to reference case. Boron reduces number of neutrons at energies around 10^{-1} eV. ^{239}Pu has a significant resonance at energy around 1 eV, therefor the effect of boron on fissions induced on ^{239}Pu is lesser than that on ^{235}U.

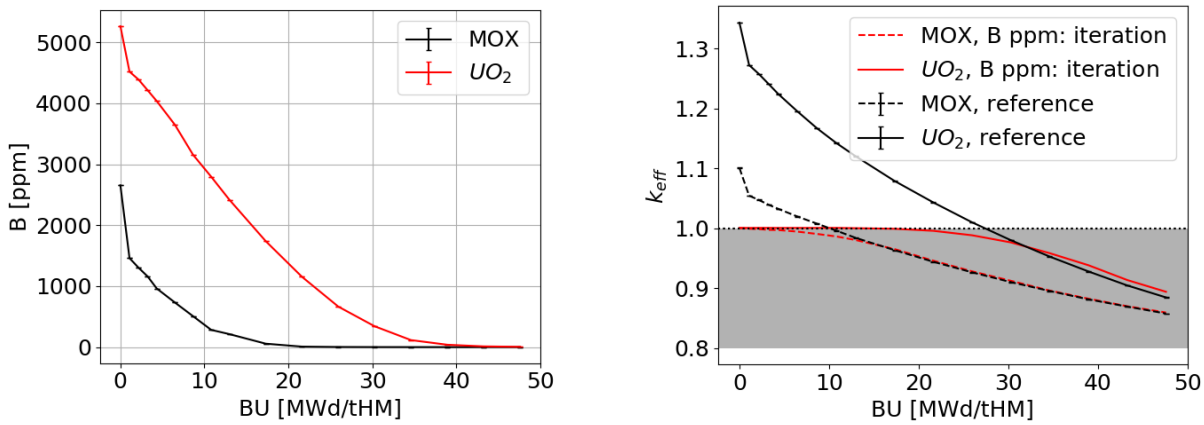

Figure 7: Concentration of boron in water (left) and neutron multiplication factor k_{eff} (right) for MOX and UO_2 fuel for semi realistic case in relation to fuel BU.

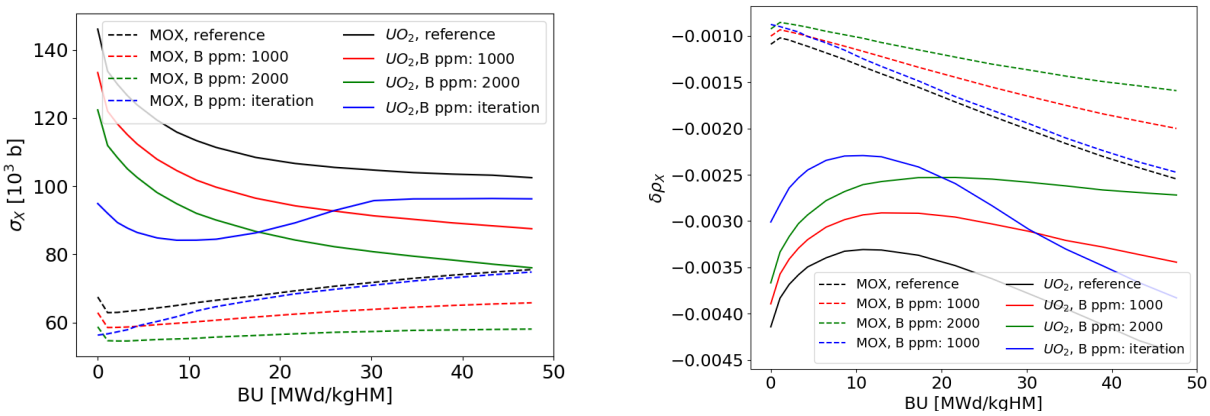

Figure 8: Neutron spectrum averaged neutron capture cross section $\bar{\sigma}_{a,X}$ in ^{135}Xe (left) and the difference between the maximum and equilibrium ^{135}Xe reactivity feedback effect $\delta\rho_X$ (right) as a function of fuel BU for UO_2 and MOX cases with 0 ppm (reference), 1000 ppm and 2000 ppm of boron.

CONCLUSION

It has been observed that from the standpoint of ^{135}Xe poisoning the MOX fuel is better for load following mode of operation than the UO_2 fuel. Negative reactivity due to ^{135}Xe build up was smaller regardless of the burnup. Higher enrichment improves the characteristics of UO_2 fuel in regards to negative reactivity due to xenon build-up after shutdown. Increasing moderator:fuel ratio increases ^{135}Xe poisoning, especially at higher burnups. Increasing boron concentration reduces ^{135}Xe poisoning. It has been observed that harder neutron spectrum and decreasing neutron flux results in less ^{135}Xe build up. If reactor needs to operate at certain power with smaller flux, then a fissile material which emits more energy than ^{235}U when fissioned is preferable, such as ^{239}Pu. That is why MOX fuel performed better than UO_2 fuel.

It is assumed that the choice of the nuclear data does not qualitatively affect the conclusions draws, even though it was studied quantitatively. ENDF/B-VII.1 library was validated numerous times also for depletion calculations and is thus deemed reliable.

Further research can be done in this field by examining different fuels, different compositions of the MOX fuel and exploring how homogeneity of the fuel affects ^{135}Xe poisoning.

ACKNOWLEDGMENTS

The research was funded by the Slovenian Research Agency (ARRS) under the grant agreement No. L2-2612.

REFERENCES

[1] B. Gjorgiev, M. Cepin, "Nuclear Power Plant Load Following: Problem Definition and Application", Proc. Int. Conf. Nuclear Energy for New Europe, Bovec, Slovenia, September 12–15, Nuclear Society of Slovenia, 2011, pp.

[2] J. Canosa, B. Harvey, "Xenon-induced oscillations", Nuclear Science and Engineering, 26, 1966,pp. 237–253

[3] J. R. Lamarsh, A. J. Baratta, Introduction to Nuclear Engineering, Prentice-Hall Inc., New Jersey, 2001, pp. 376–383

[4] Leppänen, J., et al., "The Serpent Monte Carlo code: Status, development and applications in 2013", Ann. Nucl. Energy, 82, 2015, pp. 142–150.

[5] M.B. Chadwick et al., "ENDF/B-VII.1 Nuclear Data for Science and Technology: Cross Sections, Covariances, Fission Product Yields and Decay Data", Nuclear Data Sheets, 112, 2011, pp. 2887–2996.